Received April 11, 2018, accepted May 22, 2018, date of publication May 28, 2018, date of current version June 20, 2018.

Digital Object Identifier 10.1109/ACCESS.2018.2841021

Robust Hybrid Transceiver Design for AF Relaying in Millimeter Wave Systems Under Imperfect CSI

ZHEN LUO[1], HONGQING LIU[1], (Senior Member, IEEE), YONG LI[1], (Member, IEEE), HONG WANG[2,3], AND LIN ZHANG[4]

[1]Chongqing Key Laboratory of Mobile Communications Technology, Chongqing University of Posts and Telecommunications, Chongqing 400065, China
[2]School of Communication and Information Engineering, Nanjing University of Posts and Telecommunications, Nanjing 210003, China
[3]National Mobile Communications Research Laboratory, Southeast University, Nanjing 210096, China
[4]MediaTek (Shanghai), Inc., Shanghai 200232, China

Corresponding author: Hong Wang (wanghong_1989@yahoo.com)

This work was supported in part by the Entrepreneurship and Innovation Program for Chongqing Overseas Returned Scholars under Grant Cx2017096, in part by the National Natural Science Foundation of China under Grant 61501072 and Grant 61771081, in part by the Foundation and Advanced Research Projects of Chongqing Municipal Science and Technology Commission, under Grant Cstc2015jcyjbx0009, in part by the Natural Science Foundation of Jiangsu Province under Grant BK20170910, and in part by the Open Research Foundation of National Mobile Communications Research Laboratory, Southeast University, under Grant 2018D09.

ABSTRACT In this paper, we present a robust hybrid transceiver design for millimeter-wave communication systems operating in amplify-and-forward multiple-input multiple-output relay channels. Unlike most of current works that assume the perfect or partial channel state information (CSI) at the transceivers in the design, the CSI uncertainty is taken into consideration to design a robust transceiver. To achieve that end, the average received signal-to-noise ratio (SNR) is adopted as the objective function. To produce a tractable expression, an accurate approximation of the average received SNR is derived and used as the design criterion. An alternating maximization algorithm is proposed to optimize the design criterion, in which an orthogonal matching pursuit-based algorithm is utilized to design the transceiver at the relay. Simulations show that the algorithm takes a few iterations to produce converged transceivers for the source, relay, and destination nodes. Numerical results demonstrate the substantial performance gains of the proposed scheme, compared with the existing non-robust designs.

INDEX TERMS Millimeter wave communication, MIMO, cooperative communication.

I. INTRODUCTION

The capacity of wireless networks is required to increase 1000 times by 2020 [1]. One way to meet such high demands is to exploit underutilized spectrum bands. The millimeter wave (mmWave) band offers much higher bandwidth (from 30 GHz to 300 GHz) than most present commercial wireless systems (sub 6 GHz) [2], [3]. Therefore, the mmWave wireless technology will play a key role in the next generation communication system. The main obstacle of mmWave applications is the severe propagation loss, which is orders-of-magnitude higher than the current wireless applications. Thanks to the millimeter-scale wavelength of mmWave signals, a large number of antennas can be packed at transceivers to provide significant beamforming gains via MIMO techniques. Relay and cooperative techniques can also be utilized to improve the coverage and spectral efficiency of mmWave systems.

In traditional MIMO systems, transceiver design is typically implemented in the digital domain, which can adjust both the magnitude and the phase of signals. However, in mmWave systems with large-scale antenna arrays, the high cost and power consumption of implementing one radio frequency (RF) chain per antenna element make the fully digital design infeasible. As a result, the hybrid transceiver architecture has received much consideration in mmWave systems [4]. Typically, the hybrid transceiver architecture is realized by a cascade of the analog beamformer using phase shifters and the baseband digital processor.

It is shown in [5] that the hybrid structure achieves the same performance of the fully digital beamforming if and only if the number of RF chains is twice the number of data streams. To further save the number of RF chains, various techniques have been proposed in the literature. In [6], it has been pointed out that maximizing the spectral efficiency of mmWave systems under perfect CSI assumptions can be approximated by minimizing the Euclidean distance between hybrid transceivers and fully digital processors. The design uses the sparsity of the mmWave channel and OMP algorithm, which is attractive for its low complexity. The Euclidean distance minimization problem is further investigated in [7] by incorporating the manifold optimization. In [8], the hybrid precoding designs under perfect CSI assumption that do not directly rely on the Euclidean distance approximation have been developed. The above works require the availability of perfect CSI, at least at the receiver. To relax this assumption, [9] develops an OMP algorithm based on partial channel knowledge, in which the transmitter and receiver only know its own angles of departure (AoDs) or angles of arrival (AoAs).

Relay and cooperative techniques, which have not achieved a huge success in lower frequency cellular networks, will play a more important role in improving coverage in mmWave cellular systems [2]. There is a shortage of the research in mmWave relay systems. Most of related works use the OMP-based algorithm to approximate the cascade processor with the fully digital designs under perfect CSI assumptions. In [10], the jointly hybrid transceiver design is introduced with an OMP-based sparse approximation algorithm for the half duplex AF relaying in mmWave systems. The algorithm is extended to relay networks with multiple relays in [11] and [12].

However, the implementation issues, such as bandwidth limitation, delayed feedback, estimation and quantization errors, make the perfect CSI assumption impractical. This means that transceiver designs based on imperfect CSI are vitally important. Besides, most of the fully digital designs in relay systems are developed from the mean square error (MSE) based criteria [13]–[17], which may not provide the satisfactory spectral efficiency. To make the optimization objective be more related to the spectral efficiency, SNR-based design criteria should be investigated [18]. To the best of our knowledge, the robust hybrid transceiver design in mmWave systems under imperfect CSI with SNR-based criterion has not been conducted in the literature. In this paper, we adopt the average received SNR as the objective function by taking the estimation error into consideration. Unfortunately, this objective function is difficult to produce a tractable expression. An accurate approximation of the average received SNR is derived and used as the design criterion. The accuracy of this approximation is verified by numerical simulations. We develop an alternating maximization algorithm to optimize the criterion, and an OMP-based algorithm to design the precoder at the relay. Simulations show that the algorithm only takes a few iterations to converge, which is attractive for the practical systems. It is also shown that the proposed algorithm provides a substantial performance gain compared with the existing non-robust designs.

The organization of this paper is as follows. The system and channel models used in this paper are presented in Section II. The robust hybrid design of transceivers in the relay system is presented in Section III. Simulation results are presented in Section IV before concluding the paper in Section V.

Notations: Bold lower case and upper case letters denote vectors and matrices, respectively. $(\mathbf{A})_{i,l}$ denotes the (i, l)-th entry of matrix $\mathbf{A}$; $\mathbf{a}_i$ denotes the i-th entry of vector $\mathbf{a}$. $\mathbf{A}^{(i)}$ denotes the i-th colon of matrix $\mathbf{A}$. $(\cdot)^*$, $(\cdot)^T$, $(\cdot)^H$, and $\mathrm{tr}(\cdot)$, denote the complex conjugate, matrix transpose, Hermitian transpose, and matrix trace, respectively. $\mathrm{vec}(\cdot)$ denotes the vectorization operator of a matrix which stacks the columns of the argument into a vector. $\mathbf{I}_K$ denotes the $K \times K$ identity matrix. $\mathbf{x} \sim \mathcal{CN}(\mathbf{m}, \Sigma)$ means that $\mathbf{x}$ is a circularly symmetric complex Gaussian random vector with mean $\mathbf{m}$ and covariance matrix Σ. $\|\cdot\|_F$ denotes the Frobenius norm. $E_x[\cdot]$ stands for the expectation over x. $\otimes$ denotes Kronecker product of two matrices.

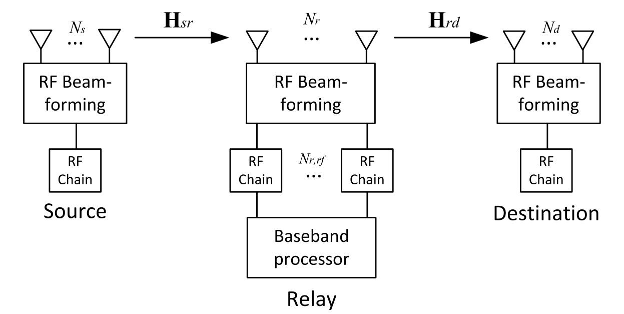

FIGURE 1. A three-node two-hop one-way relay system.

II. SYSTEM AND CHANNEL MODEL

A. SYSTEM MODEL

Consider a two-hop AF MIMO relay system as shown in Fig 1. The system consists of one source, one relay, and one destination, equipped with N_s, N_r, and N_d antennas, respectively. The source and the destination have single RF chains, and process the signal in the analog domain. The relay has $N_{r,rf}$ RF chains, and processes the signal in the analog and digital domains. The number of RF chains at the relay is subject to the constraint $N_{r,rf} \le N_r$. It is assumed that there is no direct link between the source and the destination, which is a typical two-hop relay system, particularly for the mmWave systems when the source and the destination are far away. All the nodes are half-duplex, which means that a node cannot receive and transmit signals simultaneously.

The data transmission is divided into two time slots. In the first time slot, the transmitted signals at the source terminal is sent to the relay. The received signals at the relay node are

$$\mathbf{y}_r = \sqrt{\rho_{sr}}\mathbf{H}_{sr}\mathbf{f}_s s + \mathbf{z}_{sr}, \tag{1}$$

where s is the transmitted symbol with unit variance; $\mathbf{f}_s$ is the $N_s \times 1$ RF precoder at the source, which is implemented using analog phase shifters with equal norm entries, i.e., $|\mathbf{f}_{s,i}|^2 = N_s^{-1}$; $\mathbf{y}_r$ is the received signal vector at the relay node; $\mathbf{H}_{sr}$ is the $N_r \times N_s$ channel matrix between the source and the relay; $\mathbf{z}_{sr}$ is additive complex white Gaussian noise (AWGN) vector with independent, identically distributed (i.i.d.) entries of zero mean and unit variance, i.e., $\mathbf{z}_{sr} \sim \mathcal{CN}(\mathbf{0}_{N_r\times 1}, \mathbf{I}_{N_r})$; ρ_{sr} is the total transmit power to noise ratio of the source-relay link.

In the second time slot, the relays amplify and forward the received signals to the destination, while the source keeps silent. The received signals at the destination are

$$\mathbf{y}_d = \sqrt{\rho_{rd}\rho_{sr}}\mathbf{H}_{rd}\mathbf{F}_r\mathbf{H}_{sr}\mathbf{f}_s\mathbf{s} + \sqrt{\rho_{rd}}\mathbf{H}_{rd}\mathbf{F}_r\mathbf{z}_{sr} + \mathbf{z}_{rd}, \quad (2)$$

where $\mathbf{F}_r = \mathbf{F}_{r,t}\mathbf{F}_{r,bb}\mathbf{F}_{r,r}$ with $\mathbf{F}_{r,t}$, $\mathbf{F}_{r,bb}$, and $\mathbf{F}_{r,r}$ being the $N_r \times N_{r,rf}$ analog transmit matrix, the $N_{r,rf} \times N_{r,rf}$ baseband matrix, and $N_{r,rf} \times N_r$ analog receive matrix of the hybrid processor at the relay node. $\mathbf{F}_{r,t}$ and $\mathbf{F}_{r,r}$ are implemented using analog phase shifters, i.e., for the transmit matrix $\left(\mathbf{F}_{r,t}(\mathbf{F}_{r,t})^H\right)_{i,i} = N_r^{-1}$; while $\mathbf{F}_{r,bb}$ has no hardware constraints except the total power constraint. $\mathbf{H}_{rd}$ is the $N_d \times N_r$ channel matrix between the relay and the destination; $\mathbf{z}_{rd}$ is AWGN matrix with i.i.d. entries of zero mean and unit variance, i.e., $\mathbf{z}_{rd} \sim \mathcal{CN}(\mathbf{0}_{N_d\times 1}, \mathbf{I}_{N_d})$; ρ_{rd} is the total transmit power to noise ratio of the relay-destination link.

The received signals are combined through the $N_d \times 1$ analog vector $\mathbf{w}$ at the destination. The estimated signal is given as

$$\hat{s} = \sqrt{\rho_{rd}\rho_{sr}}\mathbf{w}^H\mathbf{H}_{rd}\mathbf{F}_r\mathbf{H}_{sr}\mathbf{f}_s\mathbf{s} + \sqrt{\rho_{rd}}\mathbf{w}^H\mathbf{H}_{rd}\mathbf{F}_r\mathbf{z}_{sr} + \mathbf{w}^H\mathbf{z}_{rd}, \quad (3)$$

where $\mathbf{w}$ is implemented using analog phase shifters, i.e., $|\mathbf{w}_i|^2 = 1$.

B. CHANNEL MODEL

The mmWave propagation is shown to be limited scattering [19], [20], and well characterized by a clustered channel model, i.e., the Saleh-Valenzuela model [21]. This model expresses the mmWave channel as

$$\mathbf{H} = \frac{1}{N_{cl}N_{ray}}\sum_{i=1}^{N_{cl}}\sum_{l=1}^{N_{ray}}\alpha_{il}\mathbf{a}_r(\theta_{il})\mathbf{a}_t(\phi_{il})^H, \quad (4)$$

where N_{cl} and N_{ray} denote the number of clusters and the number of rays in each cluster; α_{il} denotes the gain of the l-th ray in the i-th cluster, which is assumed to be a complex Gaussian random variable with zero mean and variance $\sigma_{\alpha_i}^2$; $\mathbf{a}_r(\theta_{il})$ and $\mathbf{a}_t(\phi_{il})$ are the receive and transmit array response vectors, with θ_{il} and ϕ_{il} being the AoAs and AoDs, respectively.

Without loss of generality, we omit the subscript of $\mathbf{H}$ in (4) for notation simplicity. In this paper, we assume an N element uniform linear array (ULA). Nevertheless, the proposed design framework is not limited to ULA, and can be easily extended to other cases, such as uniform planar array (UPA). The array response vector $\mathbf{a}(\theta)$ of ULA is given by

$$\mathbf{a}(\theta) = \frac{1}{\sqrt{N}}\left[1, e^{j\frac{2\pi d}{\lambda}\sin(\theta)}, \ldots, e^{j(N-1)\frac{2\pi d}{\lambda}\sin(\theta)}\right]^T, \quad (5)$$

where d and λ are the antenna spacing and the signal wavelength, respectively.

In this paper, we assume that the transceivers possess only imperfect CSI. Specifically, the actual CSI can be modeled as

$$\mathbf{H}_{sr} = \hat{\mathbf{H}}_{sr} + \Delta_{sr}, \quad (6)$$

$$\mathbf{H}_{rd} = \hat{\mathbf{H}}_{rd} + \Delta_{rd}, \quad (7)$$

where $\hat{\mathbf{H}}_{sr}$ and $\hat{\mathbf{H}}_{rd}$ denote the estimated CSI of source-relay and relay-destination links available at transceivers, respectively; $\Delta_{sr} \sim \mathcal{CN}\left(\mathbf{0}, \sigma_{e,sr}^2\mathbf{I}\right)$ and $\Delta_{rd} \sim \mathcal{CN}\left(\mathbf{0}, \sigma_{e,rd}^2\mathbf{I}\right)$ denote the estimation errors in corresponding links, respectively.

III. ROBUST PRECODER DESIGN

The destination receives all the CSI, performs all the transceiver designs, and sends the design results to the source and the relay for processing. The transceivers have performance degradation because of estimation errors, if they are untreated. To remedy estimation errors, we use the approximated average received SNR for transceiver designs in this paper. This assumption is more practical than the perfect CSI assumption.

In this section, we will first present the approximation of the average received SNR, and formulate the transceiver design problem. To solve the problem, we will propose an alternating maximization algorithm to optimize the transceiver design, where an OMP-based algorithm is developed to design the transceiver at the relay.

A. DESIGN PROBLEM FORMULATION

The received SNR ρ at the destination can be expressed as

$$\rho = \frac{\rho_{rd}\rho_{sr}\|\mathbf{w}^H\mathbf{H}_{rd}\mathbf{F}_r\mathbf{H}_{sr}\mathbf{f}_s\|_F^2}{\rho_{rd}\|\mathbf{w}^H\mathbf{H}_{rd}\mathbf{F}_r\|_F^2 + \|\mathbf{w}\|_F^2}. \quad (8)$$

The average received SNR $\hat{\rho}$ is given by:

$$\hat{\rho} = E_{\mathbf{H}_{sr},\mathbf{H}_{rd}}\left[\frac{\rho_{rd}\rho_{sr}\|\mathbf{w}^H\mathbf{H}_{rd}\mathbf{F}_r\mathbf{H}_{sr}\mathbf{f}_s\|_F^2}{\rho_{rd}\|\mathbf{w}^H\mathbf{H}_{rd}\mathbf{F}_r\|_F^2 + \|\mathbf{w}\|_F^2}\right]. \quad (9)$$

However, a simple expression of $\hat{\rho}$ is very hard to obtain. Note that, for random variables a and b, the Taylor's series expansion of $E_{a,b}\left(\frac{a}{b}\right)$ can be expressed as [22]

$$E_{a,b}\left(\frac{a}{b}\right) = \frac{E_a(a)}{E_b(b)} - \frac{cov(a,b)}{E_b^2(b)} + \frac{E_a(a)var(b)}{E_b^3(b)} + \ldots \quad (10)$$

where $cov(a,b)$ and $var(b)$ are the covariance of a and b, and the variance of b, respectively. By utilizing (10), the first order Taylor's series expansion of $\hat{\rho}$, denoted by $\tilde{\rho}$, is given by

$$\tilde{\rho} = \frac{\rho_{rd}\rho_{sr}E_{\mathbf{H}_{sr},\mathbf{H}_{rd}}\left[\|\mathbf{w}^H\mathbf{H}_{rd}\mathbf{F}_r\mathbf{H}_{sr}\mathbf{f}_s\|_F^2\right]}{\rho_{rd}E_{\mathbf{H}_{rd}}\left[\|\mathbf{w}^H\mathbf{H}_{rd}\mathbf{F}_r\|_F^2\right] + \|\mathbf{w}\|_F^2}. \quad (11)$$

In Section IV, it is shown that the value of $\tilde{\rho}$ is very close to the Monte Carlo simulation of ρ. In this paper, the approximation $\tilde{\rho}$ is adopted as our optimization criterion. Based on this, a joint design of transceivers is developed as the following optimization problem

$$\begin{aligned}&\max_{\{\mathbf{f}_s,\mathbf{w},\mathbf{F}_{r,t},\mathbf{F}_{r,bb},\mathbf{F}_{r,r}\}} \tilde{\rho}\\ &\quad \text{s.t. } \mathbf{f}_s \in \mathcal{F}_s, \quad \mathbf{w} \in \mathcal{W}, \mathbf{F}_{r,t}^{(i)} \in \mathcal{F}_{r,t}, \mathbf{F}_{r,r}^{(i)} \in \mathcal{F}_{r,r},\\ &\qquad E_{\mathbf{H}_{sr}}\left[\|\mathbf{F}_{r,t}\mathbf{F}_{r,bb}\mathbf{F}_{r,r}\left(\sqrt{\rho_{sr}}\mathbf{H}_{sr}\mathbf{f}_s s + \mathbf{z}_{sr}\right)\|_F^2\right] = 1.\end{aligned} \quad (12)$$

where $\mathcal{F}_s$, $\mathcal{W}$, $\mathcal{F}_{r,t}$, and $\mathcal{F}_{r,r}$ denote the sets of the feasible RF processors induced by the equal norm entries constraints at transceiver sides of the source, the destination, and the relay, respectively. In this paper, as there are estimation errors at transceiver sides, we take the quantized response vectors in [6] as the feasible sets of the RF processors. The joint optimization of the problem (12) is known to be intractable [6]. In this paper, we will develop an alternating maximization algorithm to solve the optimization problem. With the principle of alternating maximization, we will alternately solve for $\mathbf{f}_s$, $\mathbf{w}$, and the fully digital processor $\mathbf{F}_{r,opt}$ while fixing the others. In the process, we will utilize an OMP-based algorithm to solve for $\mathbf{F}_{r,t}$, $\mathbf{F}_{r,bb}$, and $\mathbf{F}_{r,r}$ based on $\mathbf{F}_{r,opt}$.

B. TRANSCEIVER DESIGNS AT THE SOURCE AND THE DESTINATION

In the following, an iterative method is derived to solve the optimization problem (12). Firstly, we solve $\mathbf{w}$ with fixed $\mathbf{f}_s$ and $\mathbf{F}_r$. The following lemma will be used in the derivation.

Lemma 1 [23]: For random matrix $\mathbf{X} \sim \mathcal{CN}(\hat{\mathbf{X}}, \sigma^2\mathbf{I})$,

$$E_{\mathbf{X}}\left[\mathbf{X}\mathbf{A}\mathbf{X}^H\right] = \hat{\mathbf{X}}\mathbf{A}\hat{\mathbf{X}}^H + \mathrm{tr}\left(\mathbf{A}\right)\mathbf{I}, \tag{13}$$

$$E_{\mathbf{X}}\left[\mathbf{X}^H\mathbf{A}\mathbf{X}\right] = \hat{\mathbf{X}}^H\mathbf{A}\hat{\mathbf{X}} + \mathrm{tr}\left(\mathbf{A}\right)\mathbf{I}. \tag{14}$$

By applying Lemma 1, the expectations in the numerator and the denominator of (11) can be expressed as

$$\begin{aligned} &E_{\mathbf{H}_{sr},\mathbf{H}_{rd}}\left[\|\mathbf{w}^H\mathbf{H}_{rd}\mathbf{F}_r\mathbf{H}_{sr}\mathbf{f}_s\|_F^2\right] \\ &= E_{\mathbf{H}_{sr},\mathbf{H}_{rd}}\left[\mathbf{w}^H\mathbf{H}_{rd}\mathbf{F}_r\mathbf{H}_{sr}\mathbf{f}_s\mathbf{f}_s^H\mathbf{H}_{sr}^H\mathbf{F}_r^H\mathbf{H}_{rd}^H\mathbf{w}\right] \\ &= \mathbf{w}^H\Phi_1\mathbf{w}, \end{aligned} \tag{15}$$

$$\begin{aligned} &E_{\mathbf{H}_{rd}}\left[\|\mathbf{w}^H\mathbf{H}_{rd}\mathbf{F}_r\|_F^2\right] \\ &= E_{\mathbf{H}_{rd}}\left[\mathbf{w}^H\mathbf{H}_{rd}\mathbf{F}_r\mathbf{F}_r^H\mathbf{H}_{rd}^H\mathbf{w}\right] \\ &= \mathbf{w}^H\Phi_2\mathbf{w}, \end{aligned} \tag{16}$$

where

$$\Phi_1 = \hat{\mathbf{H}}_{rd}\mathbf{F}_r\Phi_3\mathbf{F}_r^H\hat{\mathbf{H}}_{rd}^H + \mathrm{tr}\left(\mathbf{F}_r\Phi_3\mathbf{F}_r^H\right)\mathbf{I}, \tag{17}$$

$$\Phi_2 = \hat{\mathbf{H}}_{rd}\mathbf{F}_r\mathbf{F}_r^H\hat{\mathbf{H}}_{rd}^H + \mathrm{tr}\left(\mathbf{F}_r\mathbf{F}_r^H\right)\mathbf{I}, \tag{18}$$

$$\Phi_3 = \hat{\mathbf{H}}_{sr}\mathbf{f}_s\mathbf{f}_s^H\hat{\mathbf{H}}_{sr}^H + \mathrm{tr}\left(\mathbf{f}_s\mathbf{f}_s^H\right)\mathbf{I}. \tag{19}$$

With fixed $\mathbf{f}_s$ and $\mathbf{F}_r$, the optimization problem (12) is simplified as

$$\begin{aligned} &\max_{\{\mathbf{w}\}} \ \frac{\mathbf{w}^H\Phi_1\mathbf{w}}{\mathbf{w}^H\Phi_2\mathbf{w}} \\ &\text{s.t. } \mathbf{w} \in \mathcal{W}. \end{aligned} \tag{20}$$

We use the exhaustive search (ES) to search for the best analog combining vector $\mathbf{w}$ at the destination. It is considered as the most straightforward search technique, while other optimization methods to save time and power consumptions are natural extensions of this work.

In a similar manner, we can design the analog precoding vector $\mathbf{f}_s$ at the source. The simplified optimization problem concerning $\mathbf{f}_s$ can be established by slightly modifying (20), and ES method is used to search for the best candidate in the feasible set $\mathcal{F}_s$. The details will not be presented here.

C. FULLY DIGITAL PROCESSOR DESIGN AT THE RELAY

Next, we solve the fully digital relay processor $\mathbf{F}_{r,opt}$ with fixed $\mathbf{f}_s$ and $\mathbf{w}$. The algorithm in the authors' previous work [24] can be utilized to solve the fully digital relay processor $\mathbf{F}_{r,opt}$. We first introduce another lemma for the derivation of the transceiver design.

Lemma 2 [25]: For matrices $\mathbf{A} \in \mathcal{C}^{m\times n}$, $\mathbf{B} \in \mathcal{C}^{n\times m}$, $\mathbf{C} \in \mathcal{C}^{n\times n}$, we have the following identities

$$\mathrm{vec}\left(\mathbf{ACB}\right) = \left(\mathbf{B}^T \otimes \mathbf{A}\right)\mathrm{vec}\left(\mathbf{C}\right), \tag{21}$$

$$\mathrm{tr}\left(\mathbf{ACB}\right) = \mathrm{vec}^H\left(\mathbf{A}^H\right)\left(\mathbf{I}_m \otimes \mathbf{C}\right)\mathrm{vec}\left(\mathbf{B}\right). \tag{22}$$

By applying Lemma 2, the terms in the numerator and the denominator of (11), and the power constraint in (12) can be modified as

$$\begin{aligned} &\mathbf{w}^H\hat{\mathbf{H}}_{rd}\mathbf{F}_r\Phi_3\mathbf{F}_r^H\hat{\mathbf{H}}_{rd}^H\mathbf{w} \\ &= \mathrm{vec}^H\left(\Phi_3^{1/2}\mathbf{F}_r^H\hat{\mathbf{H}}_{rd}^H\mathbf{w}\right)\mathrm{vec}\left(\Phi_3^{1/2}\mathbf{F}_r^H\hat{\mathbf{H}}_{rd}^H\mathbf{w}\right) \\ &= \mathrm{vec}^H\left(\mathbf{F}_r^H\right)\left[\left(\hat{\mathbf{H}}_{rd}^H\mathbf{w}\right)^*\left(\hat{\mathbf{H}}_{rd}^H\mathbf{w}\right)^T \otimes \Phi_3\right]\mathrm{vec}\left(\mathbf{F}_r^H\right), \end{aligned} \tag{23}$$

$$\begin{aligned} &\mathrm{tr}\left(\mathbf{F}_r\Phi_3\mathbf{F}_r^H\right)\mathbf{w}^H\mathbf{w} \\ &= \mathrm{vec}^H\left(\mathbf{F}_r^H\right)\left(\mathbf{w}^H\mathbf{w}\mathbf{I} \otimes \Phi_3\right)\mathrm{vec}\left(\mathbf{F}_r^H\right), \end{aligned} \tag{24}$$

$$\begin{aligned} &\mathbf{w}^H\hat{\mathbf{H}}_{rd}\mathbf{F}_r\mathbf{F}_r^H\hat{\mathbf{H}}_{rd}^H\mathbf{w} \\ &= \mathrm{vec}^H\left(\mathbf{F}_r^H\right)\left[\left(\hat{\mathbf{H}}_{rd}^H\mathbf{w}\right)^*\left(\hat{\mathbf{H}}_{rd}^H\mathbf{w}\right)^T \otimes \mathbf{I}\right]\mathrm{vec}\left(\mathbf{F}_r^H\right), \end{aligned} \tag{25}$$

$$\mathrm{tr}\left(\mathbf{F}_r\mathbf{F}_r^H\right)\mathbf{w}^H\mathbf{w} = \mathbf{w}^H\mathbf{w}\mathrm{vec}^H\left(\mathbf{F}_r^H\right)\mathrm{vec}\left(\mathbf{F}_r^H\right), \tag{26}$$

$$\begin{aligned} &E_{\mathbf{H}_{sr}}\left[\|\mathbf{F}_r\left(\sqrt{\rho_{sr}}\mathbf{H}_{sr}\mathbf{f}_s s + \mathbf{z}_{sr}\right)\|_F^2\right] \\ &= \mathrm{tr}\left[\mathbf{F}_r\left(\rho_{sr}\Phi_3 + \mathbf{I}\right)\mathbf{F}_r^H\right] \\ &= \mathrm{vec}^H\left(\mathbf{F}_r^H\right)\left[\mathbf{I} \otimes \left(\rho_{sr}\Phi_3 + \mathbf{I}\right)\right]\mathrm{vec}\left(\mathbf{F}_r^H\right). \end{aligned} \tag{27}$$

From (23)-(27), for fixed $\mathbf{f}_s$ and $\mathbf{w}$, the optimization problem for $\mathbf{F}_r$ can be modified as

$$\begin{aligned} &\max_{\{\mathbf{F}_r\}} \ \frac{\mathrm{vec}^H\left(\mathbf{F}_r^H\right)\Phi_4\mathrm{vec}\left(\mathbf{F}_r^H\right)}{\mathrm{vec}^H\left(\mathbf{F}_r^H\right)\Phi_5\mathrm{vec}\left(\mathbf{F}_r^H\right)} \\ &\text{s.t. } \mathrm{vec}^H\left(\mathbf{F}_r^H\right)\left[\mathbf{I} \otimes \left(\rho_{sr}\Phi_3 + \mathbf{I}\right)\right]\mathrm{vec}\left(\mathbf{F}_r^H\right) = 1. \end{aligned} \tag{28}$$

where

$$\Phi_4 = \left(\hat{\mathbf{H}}_{rd}^H\mathbf{w}\right)^*\left(\hat{\mathbf{H}}_{rd}^H\mathbf{w}\right)^T \otimes \Phi_3 + \mathbf{w}^H\mathbf{w}\mathbf{I} \otimes \Phi_3, \tag{29}$$

$$\Phi_5 = \left(\hat{\mathbf{H}}_{rd}^H\mathbf{w}\right)^*\left(\hat{\mathbf{H}}_{rd}^H\mathbf{w}\right)^T \otimes \mathbf{I} + \mathbf{w}^H\mathbf{w}\mathbf{I} + \mathbf{I} \otimes \left(\rho_{sr}\Phi_3 + \mathbf{I}\right). \tag{30}$$

It is noted that Φ_4 is Hermitian and Φ_5 is positive definite Hermitian. Therefore, the optimization problem (28) is a generalized Rayleigh quotient problem. By which, $\mathrm{vec}\left(\mathbf{F}_{r,opt}^H\right)$

can be solved by taking the singular value decomposition (SVD) of matrix $\Phi_5^{-H/2}\Phi_4\Phi_5^{-1/2}$, and setting

$$\mathrm{vec}\left(\mathbf{F}_{r,opt}^H\right) = \mu\Phi_5^{-1/2}\mathbf{u}_{max}, \tag{31}$$

where $\mathbf{u}_{max}$ is the eigenvector of $\Phi_5^{-H/2}\Phi_4\Phi_5^{-1/2}$ corresponding to the largest eigenvalue, μ is a scaling parameter whose value is obtained by substituting (31) into the power constraint in (28) as

$$\mu = \sqrt{\frac{1}{\mathbf{u}_{max}^H\Phi_5^{-H/2}\left[\mathbf{I}\otimes(\rho_{sr}\Phi_3+\mathbf{I})\right]\Phi_5^{-1/2}\mathbf{u}_{max}}}. \tag{32}$$

By reorganizing the elements of $\mathrm{vec}\left(\mathbf{F}_{r,opt}^H\right)$ back into the matrix structure, we obtain the fully digital relay processor $\mathbf{F}_{r,opt}$.

D. OMP-BASED HYBRID PROCESSOR DESIGN AT THE RELAY

The hybrid relay processors can be designed based on the sparse approximation. The optimization problem for minimizing the Frobenius norm of the differences between $\mathbf{F}_{r,opt}$ and the cascade of the relay processing matrices, i.e., $\mathbf{F}_{r,t}$, $\mathbf{F}_{r,bb}$, and $\mathbf{F}_{r,r}$, is written as

$$\begin{aligned}&\min_{\{\mathbf{F}_{r,t},\mathbf{F}_{r,bb},\mathbf{F}_{r,r}\}} \|\mathbf{F}_{r,opt}-\mathbf{F}_{r,t}\mathbf{F}_{r,bb}\mathbf{F}_{r,r}\|_F\\ &\quad \text{s.t. } \mathbf{F}_{r,t}^{(i)}\in\mathcal{F}_{r,t},\quad \mathbf{F}_{r,r}^{(i)}\in\mathcal{F}_{r,r},\\ &\qquad \mathrm{tr}\left[\mathbf{F}_{r,t}\mathbf{F}_{r,bb}\mathbf{F}_{r,r}(\rho_{sr}\Phi_3+\mathbf{I})\cdot\mathbf{F}_{r,r}^H\mathbf{F}_{r,bb}^H\mathbf{F}_{r,t}^H\right]=1.\end{aligned} \tag{33}$$

Define $\mathbf{A}_{r,t}$ and $\mathbf{A}_{r,r}$ as the matrices containing all elements of $\mathcal{F}_{r,t}$ and $\mathcal{F}_{r,r}$, respectively. The modified OMP-based algorithm to design the hybrid relay processors is summarized in Algorithm 1, in which the columns of $\mathbf{F}_{r,opt}$ are approximated by a linear combination of selected columns in $\mathbf{A}_{r,t}$ and $\mathbf{A}_{r,r}$, with the nonzero elements in $\mathbf{F}_{r,bb}$ specify the weights.

In steps 4, 5 and 6 of this algorithm, the column of $\mathbf{A}_{r,r}$ that correlates mostly with the residual $\mathbf{F}_{r,res}$ is selected and appended to $\mathbf{F}_{r,r}$. Then in steps 7, 8 and 9, the column of $\mathbf{A}_{r,t}$ that correlates mostly with the product of $\mathbf{F}_{r,res}$ and $\mathbf{F}_{r,r}^H$ is selected and appended to $\mathbf{F}_{r,t}$. In step 10, the baseband processor $\mathbf{F}_{r,bb}$ is obtained by solving the least squares problem $\mathbf{F}_{r,opt} = \mathbf{F}_{r,t}\mathbf{F}_{r,bb}\mathbf{F}_{r,r}$. The residual $\mathbf{F}_{r,res}$ is updated by subtracting the selected columns in step 11. The process continues until all $N_{r,rf}$ columns of $\mathbf{F}_{r,t}$ and $\mathbf{F}_{r,r}^T$ have been determined. At the end of this algorithm, the power constraint is guaranteed by step 13.

E. HYBRID TRANSCEIVER DESIGN

The hybrid transceiver design via alternating maximization is finally described in Algorithm 2. Notice that, each iteration in Algorithm 2 will increase the SNR, which has a finite value. Although the proposed method may not converge to the global optimum, it can always achieves a stationary point, and the convergence can thus be guaranteed to a local optimum. Simulation results in Section IV show that the optimization only takes few iterations to converge.

Algorithm 1 OMP-Based Algorithm to Design the Hybrid Relay Processors

Require: $\mathbf{F}_{r,opt}$, $\mathbf{A}_{r,t}$ and $\mathbf{A}_{r,r}$;

1: $\mathbf{F}_{r,t} = \mathbf{F}_{r,r} =$ Empty Matrix;
2: $\mathbf{F}_{r,res} = \mathbf{F}_{r,opt}$;
3: **for** $i \le N_{r,rf}$ **do**
4: $\quad\Gamma_{r,r} = \mathbf{F}_{r,res}\mathbf{A}_{r,r}$;
5: $\quad m = \arg\max_{i=1,\ldots,N_{cl}N_{ray}}\left(\Gamma_{r,r}^H\Gamma_{r,r}\right)_{i,i}$;
6: $\quad\mathbf{F}_{r,r} = \left[\mathbf{F}_{r,r}|\mathbf{A}_{r,r}^{(m)}\right]^T$;
7: $\quad\Gamma_{r,t} = \mathbf{A}_{r,t}^H\mathbf{F}_{r,res}\mathbf{F}_{r,r}^H$;
8: $\quad n = \arg\max_{i=1,\ldots,N_{cl}N_{ray}}\left(\Gamma_{r,t}\Gamma_{r,t}^H\right)_{i,i}$;
9: $\quad\mathbf{F}_{r,t} = \left[\mathbf{F}_{r,t}|\mathbf{A}_{r,t}^{(n)}\right]$;
10: $\quad\mathbf{F}_{r,bb} = \left(\mathbf{F}_{r,t}^H\mathbf{F}_{r,t}\right)^{-1}\mathbf{F}_{r,t}^H\mathbf{F}_{r,opt}\mathbf{F}_{r,r}^H\left(\mathbf{F}_{r,r}\mathbf{F}_{r,r}^H\right)^{-1}$;
11: $\quad\mathbf{F}_{r,res} = \frac{\mathbf{F}_{r,opt}-\mathbf{F}_{r,t}\mathbf{F}_{r,bb}\mathbf{F}_{r,r}}{\|\mathbf{F}_{r,opt}-\mathbf{F}_{r,t}\mathbf{F}_{r,bb}\mathbf{F}_{r,r}\|_F}$;
12: **end for**
13: $\mathbf{F}_{r,bb} = \frac{\mathbf{F}_{r,bb}}{\sqrt{\mathrm{tr}\left[\mathbf{F}_{r,t}\mathbf{F}_{r,bb}\mathbf{F}_{r,r}(\rho_{sr}\Phi_3+\mathbf{I})\mathbf{F}_{r,r}^H\mathbf{F}_{r,bb}^H\mathbf{F}_{r,t}^H\right]}}$;
14: **return** $\mathbf{F}_{r,t}$, $\mathbf{F}_{r,bb}$, and $\mathbf{F}_{r,r}$.

Algorithm 2 Alternating Maximization Algorithm for Hybrid Transceiver Designs

Initialization: $\mathbf{f}_{s,0}$ and $\mathbf{F}_{r,0}$, set $k=0$;

1: **repeat**
2: $\quad$Optimize $\mathbf{w}_k$ with fixed $\mathbf{f}_{s,k}$ and $\mathbf{F}_{r,k}$;
3: $\quad$Optimize $\mathbf{f}_{s,k}$ with fixed $\mathbf{w}_k$ and $\mathbf{F}_{r,k}$;
4: $\quad$Optimize $\mathbf{F}_{r,k}$ with fixed $\mathbf{w}_k$ and $\mathbf{f}_{s,k}$;
5: $\quad$set $\mathbf{F}_{r,opt} = \mathbf{F}_{r,k}$;
6: $\quad$Optimize $\mathbf{F}_{r,t,k}$, $\mathbf{F}_{r,bb,k}$, and $\mathbf{F}_{r,r,k}$ using Algorithm 1 based on $\mathbf{F}_{r,opt}$;
7: **until** a stopping criterion triggers

IV. NUMERICAL RESULTS

In this section, we numerically evaluate the performance of the proposed method. We model the propagation channels as a $N_{cl} = 8$ cluster environment with $N_{ray} = 10$ rays per cluster. For simplicity of exposition, we assume all clusters are of equal power, i.e., $\sigma_{\alpha_i}^2 = 1, \forall i$. The azimuth AoAs and AoDs follow Laplacian distribution with uniformly distributed means over $[0, 2\pi)$ and angular spread 10 degrees. The antenna elements in the ULA are separated by a half wavelength distance, i.e., $d = \lambda/2$. The transmitted SNRs and the powers of estimation errors for the source-relay and relay-destination links are set to be equal, i.e., $\rho_{sr} = \rho_{rd}$ and $\sigma_{e,sr} = \sigma_{e,rd} = \sigma_e$. All the reported results are averaged over 5000 random channel realizations. The stopping criterion of Algorithm 2 is chosen that the increasing SNR in each iteration is below 1×10^{-6}.

In Fig 2, we plot the spectral efficiencies versus transmitted SNRs for different estimation error settings.

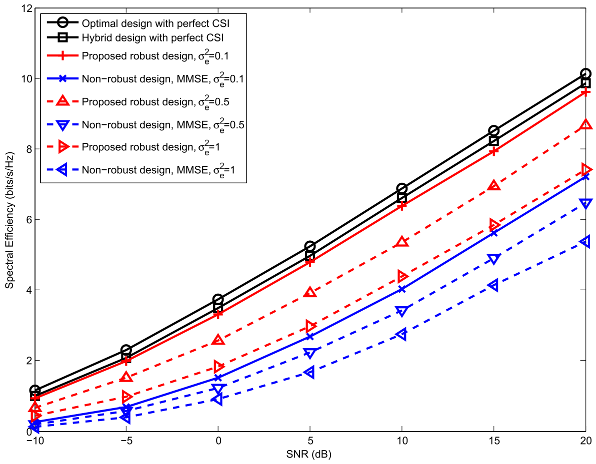

FIGURE 2. Spectral efficiencies versus transmitted SNRs with $N_s = N_d = 8$, $N_r = 16$, $N_{r,rf} = 4$.

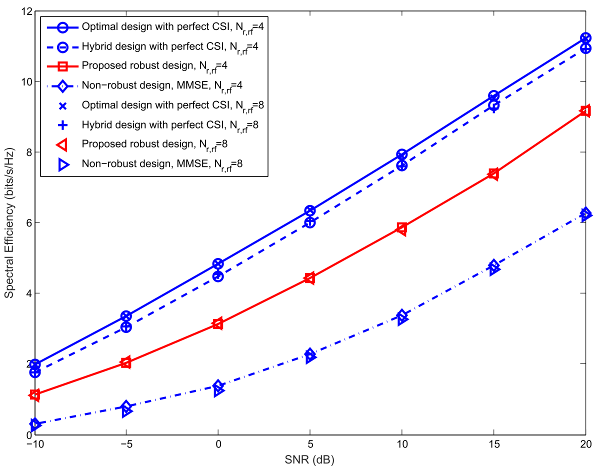

FIGURE 3. Spectral efficiencies versus transmitted SNRs with $N_s = N_d = 16$, $N_r = 32$, $\sigma_e^2 = 1$.

For comparison, we also include the average rates of the optimal fully digital processor under perfect CSI, the hybrid processor under perfect CSI, and the non-robust minimal mean square error (MMSE) based design [12]. Configurations of $N_s = N_d = 8$, $N_r = 16$, $N_{r,rf} = 4$ are considered. As shown in the figure, the optimal fully digital processor produces the best rates. The hybrid processor achieves spectral efficiencies that are within a small gap from the optimality. The above two designs are performed under the proposed structure with perfect CSI assumption, which cannot be obtained in practice. The proposed robust transceiver design provides substantial gains over the non-robust MMSE-based design in [12] for all SNRs. Furthermore, with the decreasing of the power of estimation error, the proposed design approaches the hybrid processor with perfect CSI as expected.

In Fig 3, we plot the spectral efficiencies with different RF chains at the relay. Configurations of $N_s = N_d = 16$, $N_r = 32$, $\sigma_e^2 = 1$ are considered. The optimal fully digital processor with perfect CSI is still the best. The small gap from the optimality can be seen for the hybrid processor with perfect CSI. The proposed robust transceiver design outperforms the non-robust MMSE-based design. However, because we consider only one stream in the system, increasing the number of RF chains at the relay does not provide further gains for the hybrid design. The designs for multi-stream is the future direction of this work.

TABLE 1. The computational complexity of matrix operations required per iteration for different hybrid transceiver designs.

Matrix operations	Hybrid design with perfect CSI	Non-robust design, MMSE	Proposed scheme
Multiplication	$O(N_r^4)$	$O(N_d N_r N_s)$	$O(N_r^4)$
Inversion	$O(N_r^6)$	$O(N_d^3 + N_s^3)$	$O(N_r^6)$
SVD	$O(N_r^6)$	$O(N_d N_r^2 + N_r N_s^2)$	$O(N_r^6)$

TABLE 2. The average iteration numbers for the proposed method to converge to a solution.

SNR	Scenario I	Scenario II	Scenario III
-10dB	3.375	3.418	3.452
-5dB	3.411	3.427	3.406
0dB	3.363	3.383	3.500
5dB	3.365	3.378	3.428
10dB	3.395	3.374	3.466
15dB	3.413	3.397	3.450
20dB	3.387	3.404	3.438

In the next, we compare the computational complexity of different hybrid designs, i.e., the proposed design, the design with perfect CSI, and the non-robust MMSE-based design. As the OMP-based algorithm is required in all these schemes, we list the computational complexity of matrix operations required per iteration exclude the OMP-based algorithm in Table 1. As we can see, the computational complexities of the hybrid design with perfect CSI and the proposed scheme are in the same order, and both of them are dominated by the matrix inversions and SVD operations. As the matrix dimensions introduced by the Kronecker product in these two schemes are larger than the MMSE-based design, the computational complexities of the first two are higher than the latter one. However, the hybrid design with perfect CSI and the proposed scheme can provide significant gains in spectral efficiency compared with the MMSE-based design as shown in Fig 2 and 3. Combined with the difficulty of perfect CSI acquisition, the proposed design is more attractive than other existing schemes in practice.

Fig 4 evaluates the accuracy of the approximation in (11). For the evaluation, we generate power of the estimation error randomly for each channel realization. The configurations are $N_s = N_d = 16$, $N_r = 32$, $N_{r,rf} = 8$ for Scenario I; $N_s = N_d = 16$, $N_r = 32$, $N_{r,rf} = 4$ for Scenario II; and $N_s = N_d = 8$, $N_r = 16$, $N_{r,rf} = 4$ for Scenario III, respectively. The received SNR in (8) and the first order Taylor's series expansion in (11) are averaged over 5000 random channel realizations. It is shown that the value of $\tilde{\rho}$ in (11) is very close to the Monte Carlo simulation of ρ in (8) for different configurations. The results demonstrate that the proposed objective function is an accurate approximation of the average received SNR for transceiver designs. In Table 2, the average iteration numbers for the proposed method to converge to a solution

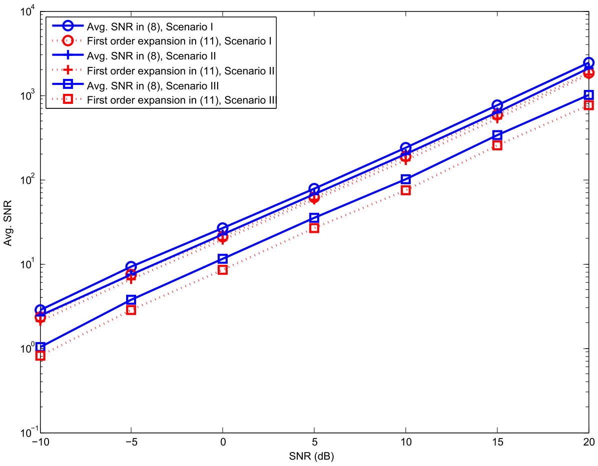

FIGURE 4. **Comparison of the average received SNR and the first order Taylor's series expansion in (10). Scenario I: $N_s = N_d = 16$, $N_r = 32$, $N_{r,rf} = 8$; Scenario II: $N_s = N_d = 16$, $N_r = 32$, $N_{r,rf} = 4$; Scenario III: $N_s = N_d = 8$, $N_r = 16$, $N_{r,rf} = 4$.**

have been listed for simulations in Fig 4. It is seen that it takes less than 4 iterations for all the simulations, which means that the proposed method converges very fast.

V. CONCLUSIONS

The robust hybrid transceiver design for mmWave AF MIMO relay system is presented by taking the estimation error into consideration. An accurate approximation of the average received SNR is derived and used as the design criterion. The value of the approximated SNR is shown to be very close to the simulated value by the Monte-Carlo method for different configurations, justifying its use as the design criterion. An alternating maximization algorithm is proposed to optimize the design criterion, in which an OMP-based algorithm is utilized to design the precoder at the relay. Numerical results show that the algorithm takes a few iterations to converge, and provides substantial performance gains over the existing non-robust designs.

REFERENCES

[1] J. G. Andrews *et al.*, "What will 5G be?" *IEEE J. Sel. Areas Commun.*, vol. 32, no. 6, pp. 1065–1082, Jun. 2014.

[2] R. W. Heath, Jr., N. González-Prelcic, S. Rangan, W. Roh, and A. M. Sayeed, "An overview of signal processing techniques for millimeter wave MIMO systems," *IEEE J. Sel. Topics Signal Process.*, vol. 10, no. 3, pp. 436–453, Apr. 2016.

[3] J. G. Andrews, T. Bai, M. N. Kulkarni, A. Alkhateeb, A. K. Gupta, and R. W. Heath, Jr., "Modeling and analyzing millimeter wave cellular systems," *IEEE Trans. Commun.*, vol. 65, no. 1, pp. 403–430, Jan. 2017.

[4] S. Han, C.-L. I, Z. Xu, and C. Rowell, "Large-scale antenna systems with hybrid analog and digital beamforming for millimeter wave 5G," *IEEE Commun. Mag.*, vol. 53, no. 1, pp. 186–194, Jan. 2015.

[5] X. Zhang, A. F. Molisch, and S.-Y. Kung, "Variable-phase-shift-based RF-baseband codesign for MIMO antenna selection," *IEEE Trans. Signal Process.*, vol. 53, no. 11, pp. 4091–4103, Nov. 2005.

[6] O. El Ayach, S. Rajagopal, S. Abu-Surra, Z. Pi, and R. W. Heath, Jr., "Spatially sparse precoding in millimeter wave MIMO systems," *IEEE Trans. Wireless Commun.*, vol. 13, no. 3, pp. 1499–1513, Mar. 2014.

[7] X. Yu, J.-C. Shen, J. Zhang, and K. B. Letaief, "Alternating minimization algorithms for hybrid precoding in millimeter wave MIMO systems," *IEEE J. Sel. Topics Signal Process.*, vol. 10, no. 3, pp. 485–500, Apr. 2016.

[8] F. Sohrabi and W. Yu, "Hybrid digital and analog beamforming design for large-scale antenna arrays," *IEEE J. Sel. Topics Signal Process.*, vol. 10, no. 3, pp. 501–513, Apr. 2016.

[9] A. Alkhateeb, O. El Ayach, G. Leus, and R. W. Heath, Jr., "Hybrid precoding for millimeter wave cellular systems with partial channel knowledge," in *Proc. Inf. Theory Appl. Workshop (ITA)*, Feb. 2013, pp. 1–5.

[10] J. Lee and Y. H. Lee, "AF relaying for millimeter wave communication systems with hybrid RF/baseband MIMO processing," in *Proc. IEEE Int. Conf. Commun. (ICC)*, Jun. 2014, pp. 5838–5842.

[11] H. Abbas and K. Hamdi, "Millimeter wave communications over relay networks," in *Proc. IEEE Wireless Commun. Netw. Conf. (WCNC)*, Mar. 2017, pp. 1–5.

[12] H. Abbas and K. Hamdi, "Hybrid beamformers design for MIMO relay networks in millimeter wave," in *Proc. IEEE Wireless Commun. Netw. Conf. (WCNC)*, Mar. 2017, pp. 1–6.

[13] C. Xing, S. Ma, and Y.-C. Wu, "Robust joint design of linear relay precoder and destination equalizer for dual-hop amplify-and-forward MIMO relay systems," *IEEE Trans. Signal Process.*, vol. 58, no. 4, pp. 2273–2283, Apr. 2010.

[14] Y. Rong, "Robust design for linear non-regenerative MIMO relays with imperfect channel state information," *IEEE Trans. Signal Process.*, vol. 59, no. 5, pp. 2455–2460, May 2011.

[15] Y. Fu, L. Yang, W.-P. Zhu, and C. Liu, "Optimum linear design of two-hop MIMO relay networks with QoS requirements," *IEEE Trans. Signal Process.*, vol. 59, no. 5, pp. 2257–2269, May 2011.

[16] L. Gopal, Y. Rong, and Z. Zang, "Robust MMSE transceiver design for nonregenerative multicasting MIMO relay systems," *IEEE Trans. Veh. Technol.*, vol. 66, no. 10, pp. 8979–8989, Oct. 2017.

[17] H. Wang, R. Zhang, R. Song, and S.-H. Leung, "A novel power minimization precoding scheme for MIMO-NOMA uplink systems," *IEEE Commun. Lett.*, vol. 22, no. 5, pp. 1106–1109, May 2018.

[18] X. Xie, H. Yang, and A. V. Vasilakos, "Robust transceiver design based on interference alignment for multi-user multi-cell MIMO networks with channel uncertainty," *IEEE Access*, vol. 5, pp. 5121–5134, Apr. 2017.

[19] T. S. Rappaport *et al.*, "Millimeter wave mobile communications for 5G cellular: It will work!" *IEEE Access*, vol. 1, pp. 335–349, May 2013.

[20] T. S. Rappaport, F. Gutierrez, Jr., E. Ben-Dor, J. N. Murdock, Y. Qiao, and J. I. Tamir, "Broadband millimeter-wave propagation measurements and models using adaptive-beam antennas for outdoor urban cellular communications," *IEEE Trans. Antennas Propag.*, vol. 61, no. 4, pp. 1850–1859, Apr. 2013.

[21] T. S. Rappaport, R. W. Heath, Jr., R. C. Daniels, and J. N. Murdock, *Millimeter Wave Wireless Communications*. New York, NY, USA: Pearson Education, 2014.

[22] A. Papoulis and S. U. Pillai, *Probability—Random Variables and Stochastic Processes*. New York, NY, USA: McGraw-Hill, 1991.

[23] A. K. Gupta and D. K. Nagar, *Matrix Variate Distributions*. London, U.K.: Chapman & Hall, 2000.

[24] Z. Luo, S. H. Leung, and X. Yu, "Robust precoder design for MIMO relay networks over double correlated Rician channels," *IEEE Trans. Signal Process.*, vol. 63, no. 9, pp. 2295–2305, May 2015.

[25] J. W. Brewer, "Kronecker products and matrix calculus in system theory," *IEEE Trans. Circuits Syst.*, vol. CAS-25, no. 9, pp. 772–781, Sep. 1978.

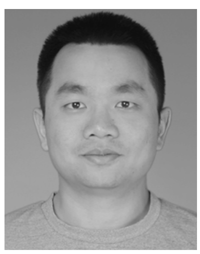

ZHEN LUO received the B.Eng. and M.Sc. degrees in control science and engineering from the Harbin Institute of Technology, Harbin, in 2005 and 2009, respectively, and the Ph.D. degree in electronic engineering from the City University of Hong Kong, Hong Kong, in 2014. From 2014 to 2015, he was a Senior Research Associate with the Department of Electronic Engineering, City University of Hong Kong. From 2015 to 2016, he was a Post-Doctoral Fellow with the Department of Electronic and Computer Engineering, The Hong Kong University of Science and Technology, Hong Kong. Since 2016, he has been with the Chongqing Key Laboratory of Mobile Communications Technology, Chongqing University of Posts and Telecommunications, Chongqing, China. His current research interests are cooperative communication in MIMO networks, channel estimation, and millimeter-wave communication.

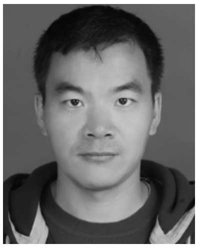

HONGQING LIU (M'15–SM'17) received the bachelor's and master's degrees from Xidian University, Xi'an, China, in 2003 and 2006, respectively, and the Ph.D. degree from the City University of Hong Kong, Hong Kong, in 2009, all in electronic engineering. In 2009, he joined the Acoustic Research Laboratory, National University of Singapore, as a Research Fellow. Since 2013, he has been with the School of Information and Communication Engineering, Chongqing University of Posts and Telecommunications, as a Faculty Member. His research interests lie in the areas of statistical signal processing and convex optimization, including sparse recovery, localization/tracking, and parameter estimation.

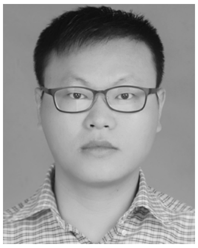

YONG LI (S'11–M'13) received the B.Sc. degree in electronic and information engineering from the Chongqing University of Posts and Telecommunications (CQUPT), Chongqing, China, in 2003, and the M.S. and Ph.D. degrees in communication engineering from Xiamen University, Fujian, China, in 2006 and 2012, respectively. From 2006 to 2007, he was a Research Assistant with the Department of Electronic Engineering, City University of Hong Kong, Hong Kong. From 2007 to 2009, he was with Gallop Gear Co. Ltd., Chongqing. From 2011 to 2012, he was with the University of California at Davis, Davis, CA, USA, as a Visiting Scholar. Since 2013, he has been with CQUPT, where he is currently an Associate Professor with the Key Laboratory of Mobile Communication. He has authored over 20 papers in peer-reviewed journals or conference proceedings and held two granted national patents. His research interests include channel coding, MIMO-OFDM, joint blind equalization and decoding, and distributed storage coding.

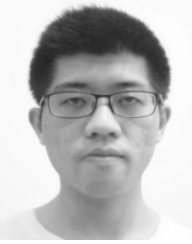

HONG WANG received the B.S. degree in telecommunications engineering from Jiangsu University, Zhenjiang, China, in 2011, and the Ph.D. degree from the Department of Telecommunications Engineering, Nanjing University of Posts and Telecommunications (NUPT), Nanjing, China, in 2016. From 2014 to 2015, he was a Research Assistant with the Department of Electronic Engineering, City University of Hong Kong, Hong Kong, where he was a Senior Research Associate with the State Key Laboratory of Millimeter Waves from 2016 to 2018. Since 2016, he has been an Instructor with the Department of Telecommunication Engineering, NUPT. His research interests are in the area of broadband wireless communication, particularly in interference analysis and management in HetNets.

LIN ZHANG received the B.Eng. degree from Shandong University, Jinan, in 2006, and the Ph.D. degree in electronic engineering from Peking University, Beijing, in 2012. From 2012 to 2014, he was a Post-Doctoral Fellow with the Department of Electronic Engineering, City University of Hong Kong, Hong Kong. Since 2014, he has been with Mediatek (Shanghai), Inc., as a Physical-Layer Algorithm Design Architect. His current research interest is in high-performance/reliable algorithm design on chip for LTE/NBIOT/5G.